Sponsors

Body-Motion Driven MEMS Generator for Implantable Biomedical Devices

Jose Martinez-Quijada, Sazzadur Chowdhury
Research Centre for Integrated Microsystems (RCIM)
University of Windsor
Windsor, Ontario

Abstract

- A MEMS-based axial flux power generator for implantable biomedical devices has been presented
- In the system, a semicircular magnetic pendulum oscillates around a central shaft due to the physiological motion of the body organs to induce a voltage across an underlying copper coil
- The 1.0 mm^2 footprint area device can generate 390 μW RMS power with an open circuit RMS voltage of 1.1 volts
- A number of microgenerators could be stacked vertically or horizontally or a scaled up version can be used if greater amount of power is needed
- The device can provide a greater energy supply per unit volume at a much smaller size and weight and maintenance free longer life compared to conventional batteries
- In this paper, an optimized microgenerator design for cardiac pace maker application has been presented

Device Operating Principle

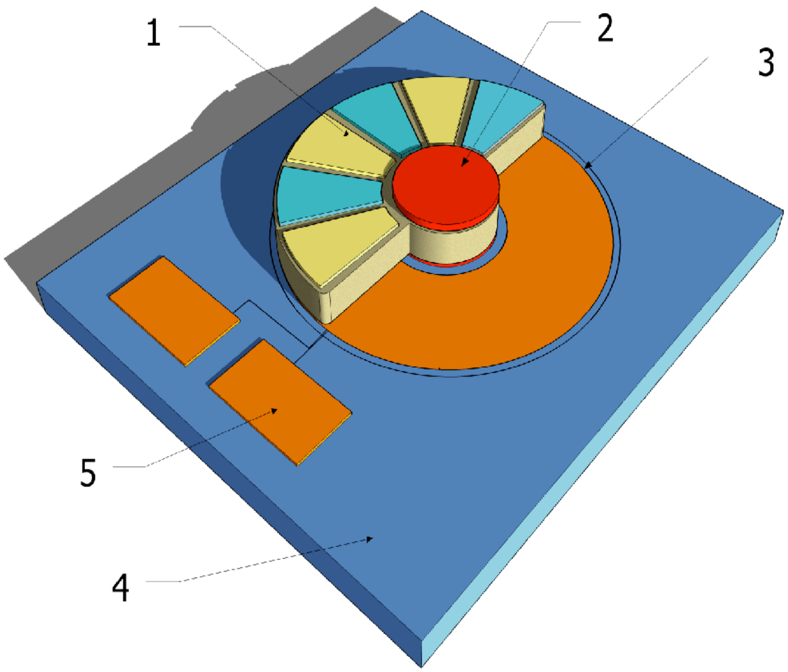

- When the asymmetrical pendulum leaves its initial stable position due to the motion of some body organ, it oscillates for a certain time to finally reach a new stable position
- In the process, a changing axial magnetic field cutting through the underneath planar copper coil induces a voltage across its terminals

1. NdFeB embedded SU-8 magnetic pendulum rotor
2. Shaft
3. Square cross-section planar copper coil
4. Substrate
5. Contact pads

Device Operating Principle

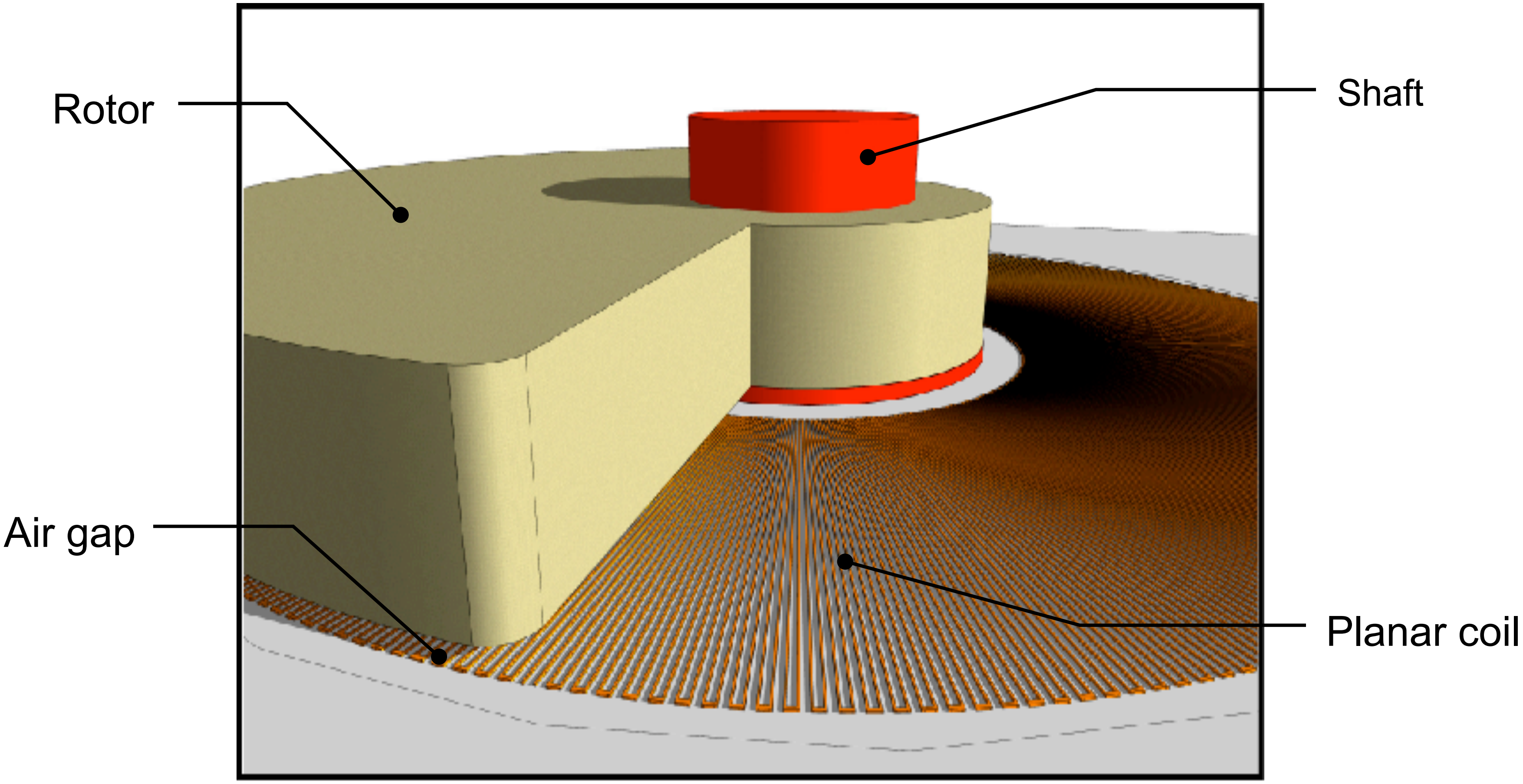

Close Up View of the Microgenerator

Rotor Oscillation

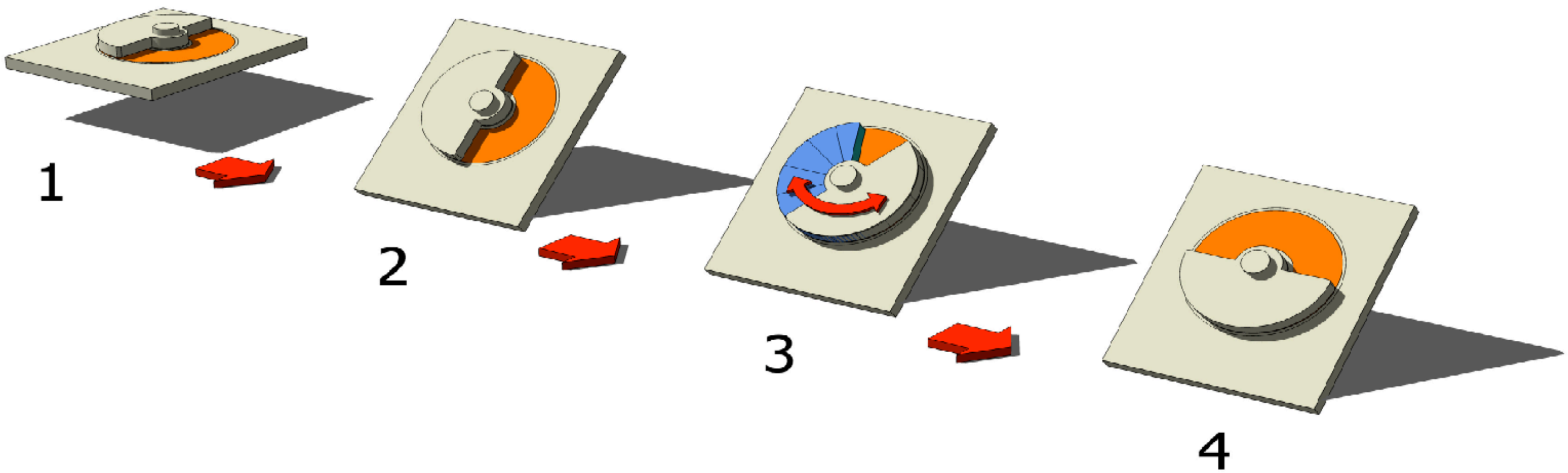

1. Initial stable state
2. Excitation
3. Oscillation
4. New stable state

Key Advantages

- A non-toxic clean energy source
- No fluid/gas injection or emissions
- No elastically deformable structures
- Can be completely sealed and shielded in a biocompatible capsule
- High energy density per unit volume
- Much smaller/lighter than existing pacemaker batteries
- Free of self-discharge phenomenon
- Stackable/Scalable to meet higher power demands
- Smaller volume means smaller foreign material inside the body
- Implantation is not restricted to a specific area
- Power generation at any physical posture of a person
- Minimizes frequency of invasive surgery

Target Applications

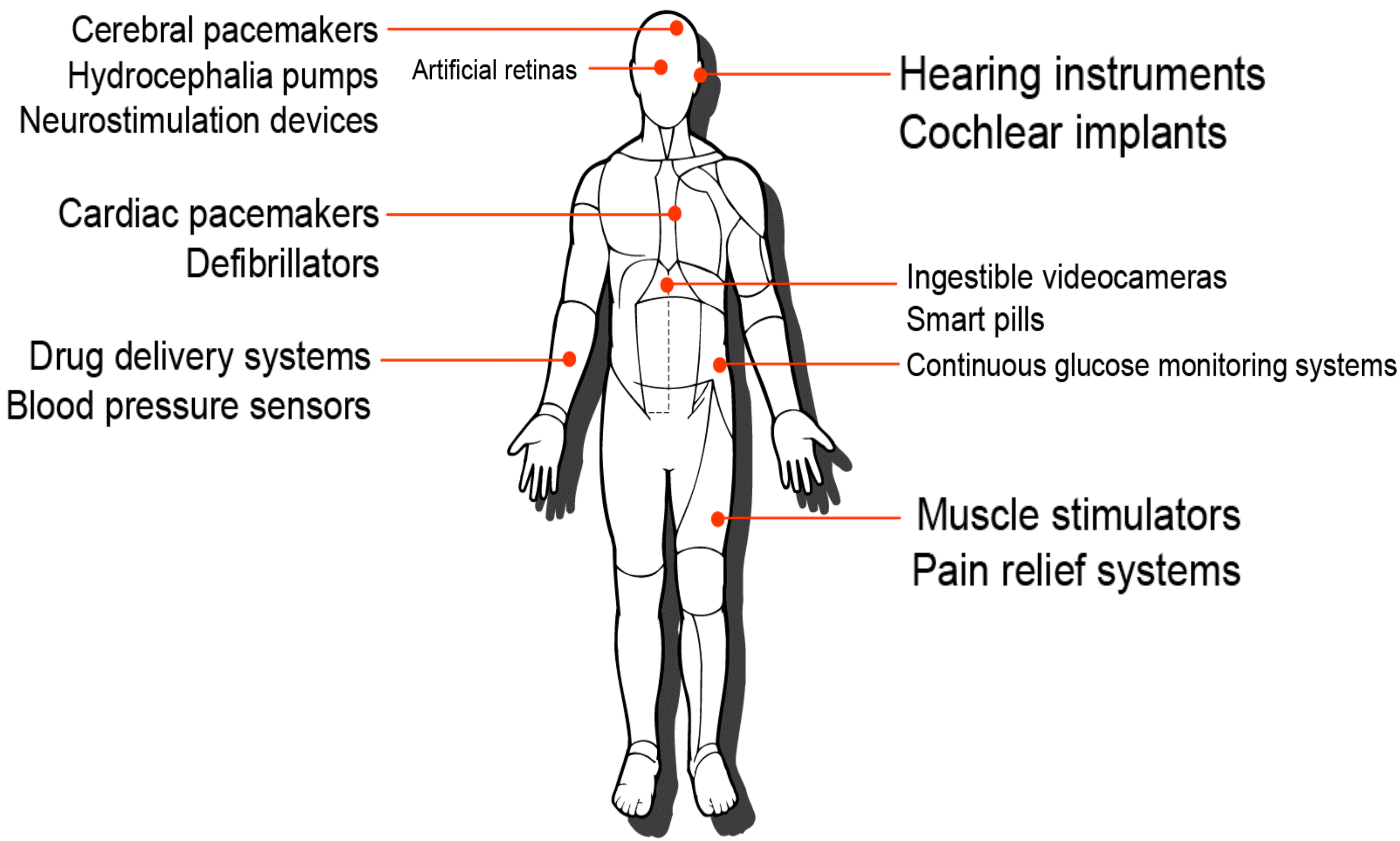

Excitation and Conduction System of Human Heart

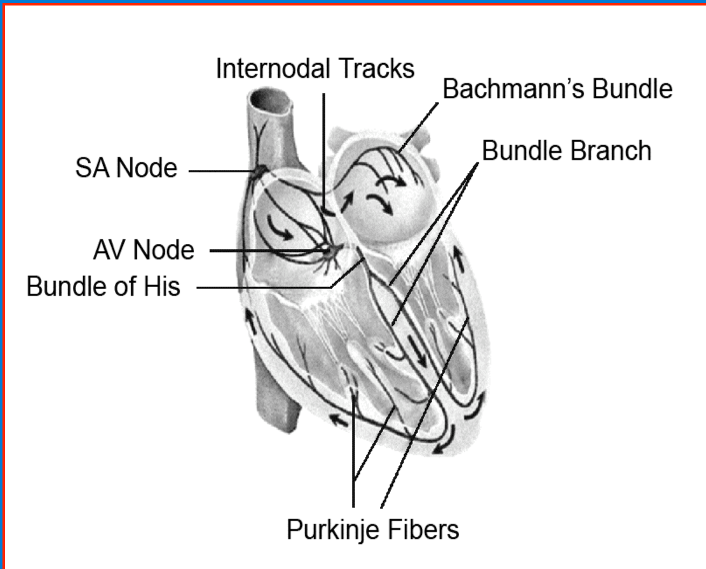

- During normal sinus rhythm, the heart is controlled by the Sinoatrial (SA) node (60–100 bpm)
- The right atrial internodal tracks and Bachmann's bundle conduct the SA-nodal activation throughout the atria, initiating a coordinated contraction of the atrial walls
- The atrial wall contraction then transfers through the atrioventricular (AV) node
- The Bundle of His then transfers the impulse at a high velocity while splitting the excitation throughout the two ventricles, enabling a coordinated and massive contraction (Ref. [5])

Pacemaker Function

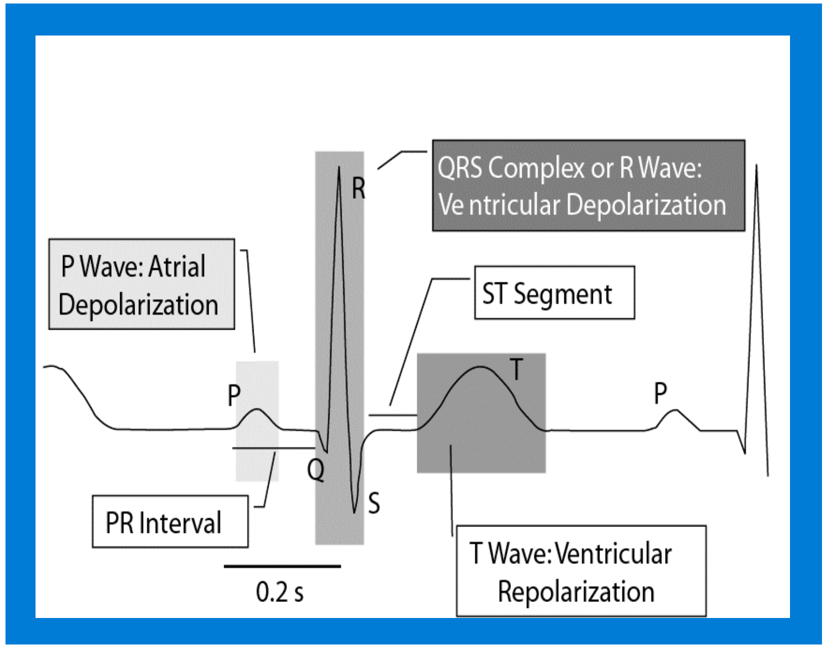

- Arrhythmia entails the abnormal or irregular beating rhythm of the heart due to asynchrony of the cardiac chambers
- A pacemaker is used to restore synchrony between the atria and ventricles by applying controlled electrical pulses to the heart muscles.

Pacemaker Power Supply: Major Requirements

- For effective pacing, the output pulse should have an appropriate width and sufficient energy to depolarize the myocardial cells close to the electrode
- Many factors affect the longevity of the battery, including primary device settings like pulse amplitude and duration and pacing rate (Ref. [5])

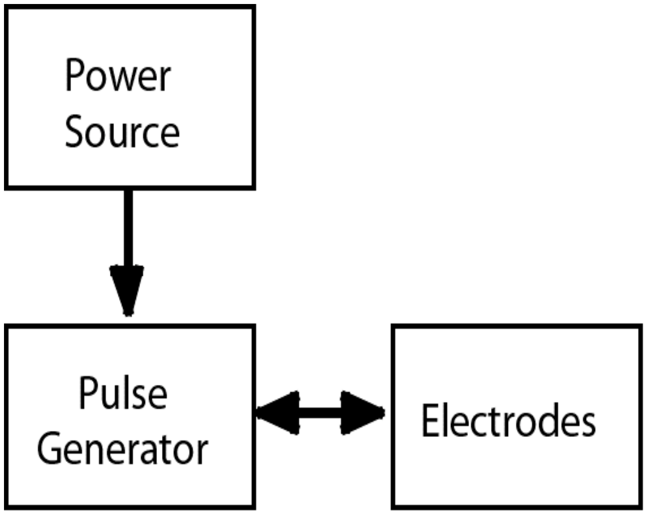

A typical pacemaker configuration

(Ref. [2])

Typical Commercial Pacemaker Battery Specifications

- Open circuit voltage: 3.0 Volt
- Control circuit minimal voltage: 2.2 Volt
- Control circuit current drain: 10 μA
- Duty cycle: 16.7 %
- Ampere-hour (Ah rating): 2 Ah (typical rating)
- Energy per pulse: 3-6 μJ
- Volume occupied: 5–8 cc
- Effective lifetime: 5 to 7 years

The MEMS microgenerator has been designed to meet the above electrical specifications

Design Methodology

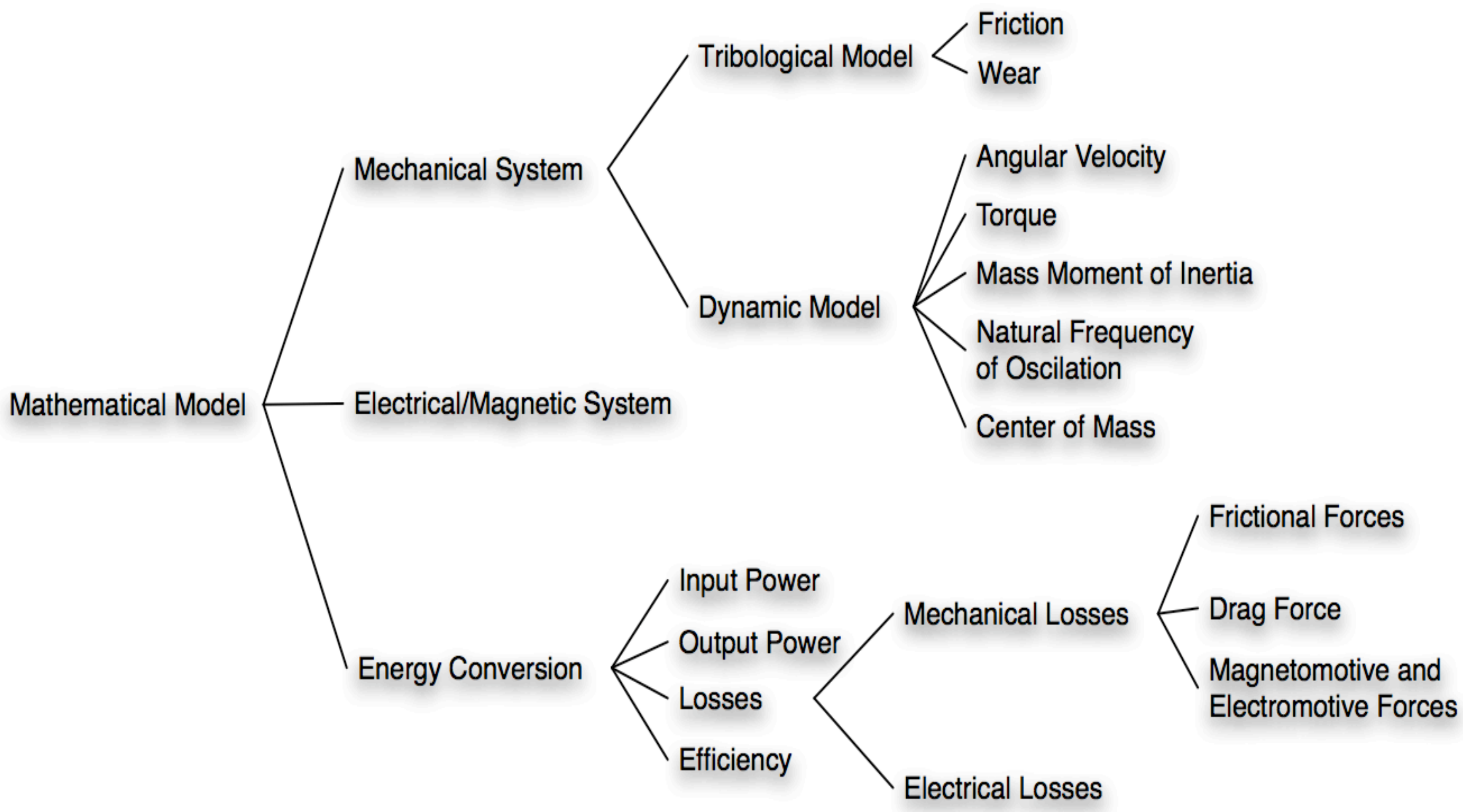

Mathematical Modeling

Induced voltage:

$$V_{rms} = 2\beta\sqrt{2}\,N_p^2\,\Omega\,N_t\,B\,S$$

Generated power:

$$P = \frac{V_{rms}^2}{R}$$

Angular velocity:

$$\Omega = \frac{4\sqrt{3}}{3}\sqrt{\frac{g\sin(\theta)}{Rp\,\pi}}$$

N_p	Number of magnetic pole pairs in the pendulum shaped rotor
N_t	Number of turns exposed directly to a changing magnetic field
B	Magnetic flux density of the air gap
S	Exposed face area
Ω	Rotor angular velocity
β	Shape factor
R	Coil resistance
Rp	Radius of pendulum shaped rotor
θ	Angular displacement

(Ref. [4])

Mathematical Modeling

Shape factor: $$\beta = \frac{T_{pm}}{T_{pm} + T_{cl} + T_{ag}}$$

Magnetic flux density of the air gap: $$B = \beta \cdot Br$$

T_{pm} Thickness of permanent magnets
T_{cl} Thickness of coil layer
T_{ag} Thickness of the air gap
Br Remanence of the permanent magnets

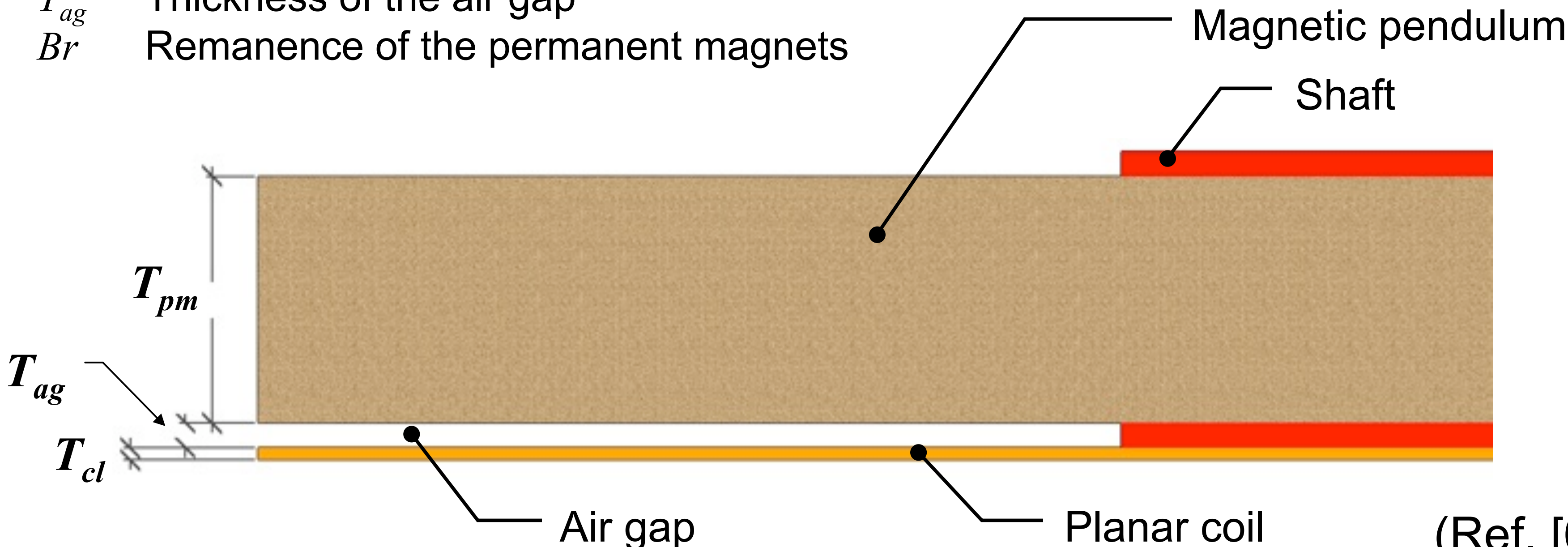

(Ref. [6])

Magnetization of Pendulum Rotor

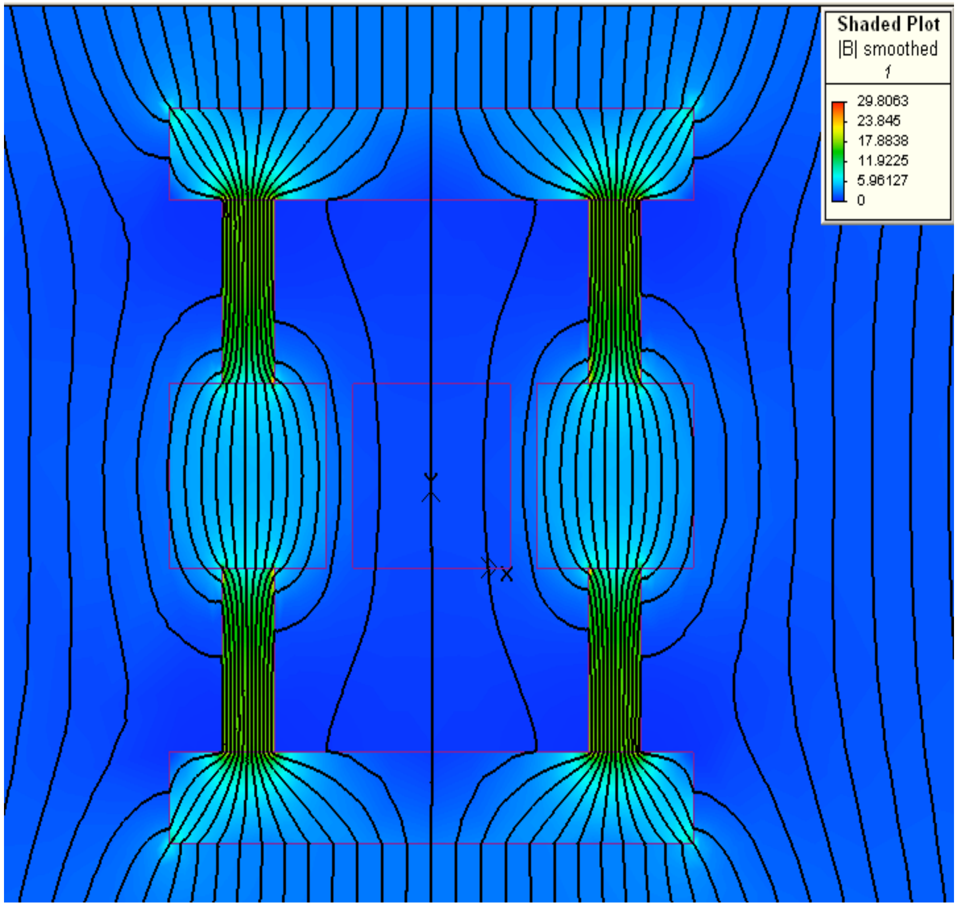

Alternate polarities of NdFeB micromagnets produced by Magnetic Flux Shielding

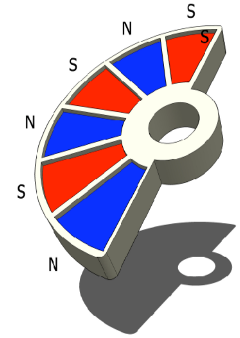

Detail of the Magnetic Pendulum

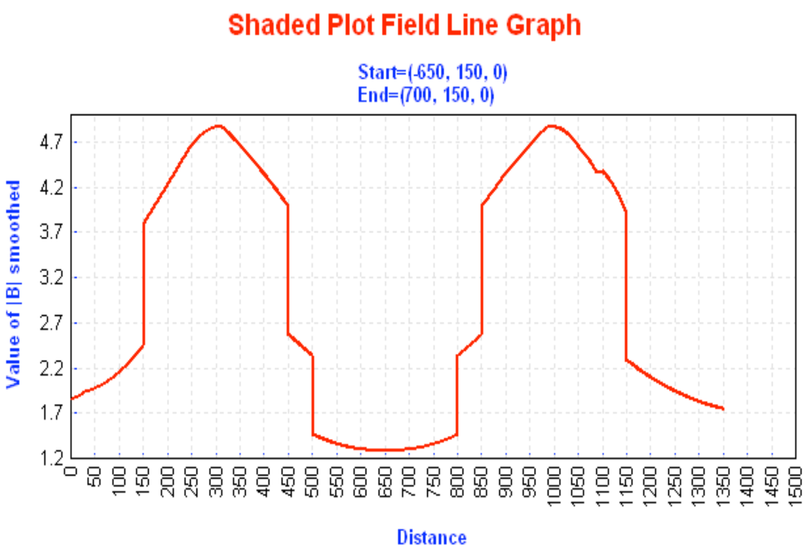

Magnetic flux density during magnetization

Friction Between the Rotor and the Shaft

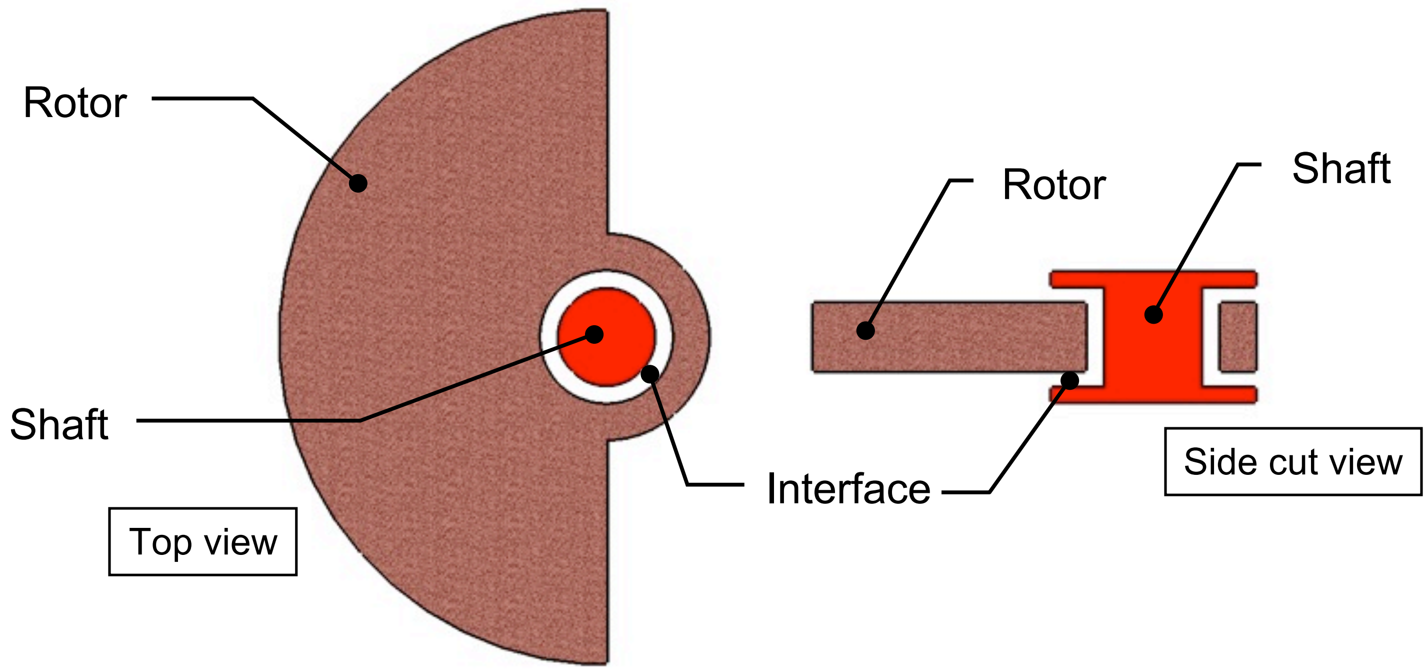

- During operation frictional forces and wear occur at interfacing surfaces of the SU-8 rotor and the shaft.
- A bearing mechanism is necessary to minimize energy losses and excesive wear of the rotor and the shaft.
- A nanotechnology based lubrication system has been chosen instead of conventional microbearings to minimize frictional forces and wear.

Lubrication Mechanisms of IF-WS_2 Nanoparticles

- Inorganic Fullerene-like Tungsten disulphide (IF-WS_2) nanoparticles blended with a Ni-P alloy are electroless deposited
- During friction, IF-WS_2 particles are slowly released from the Ni-P alloy and serve as sliding spacers between the rotor and the shaft
- Prevent contact between asperities of surfaces and facilitate the removal of wear debris from interface, limiting abrasive wear
- Exfoliation of particles: one-atom thick sheets produce superlubricity effect. (Ref. [7])

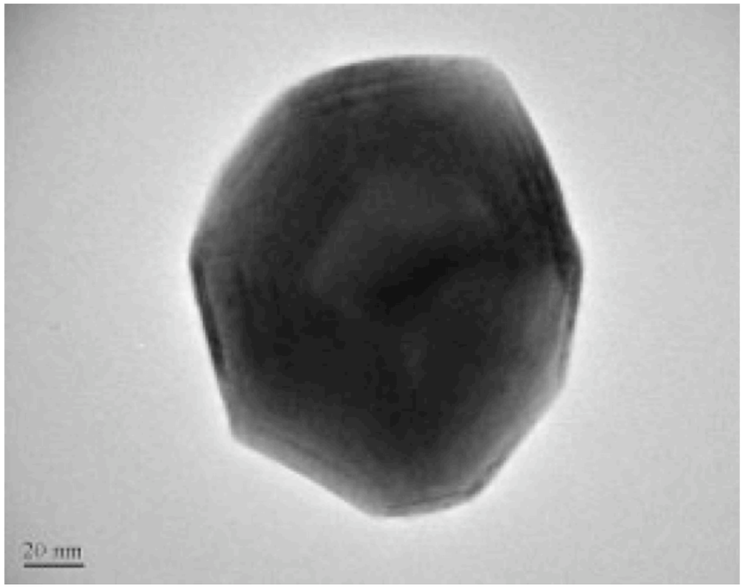

Fullerane-like IF-WS_2 Nanoparticle

(100 nm wide)

Nanotechnology-Based Lubrication System

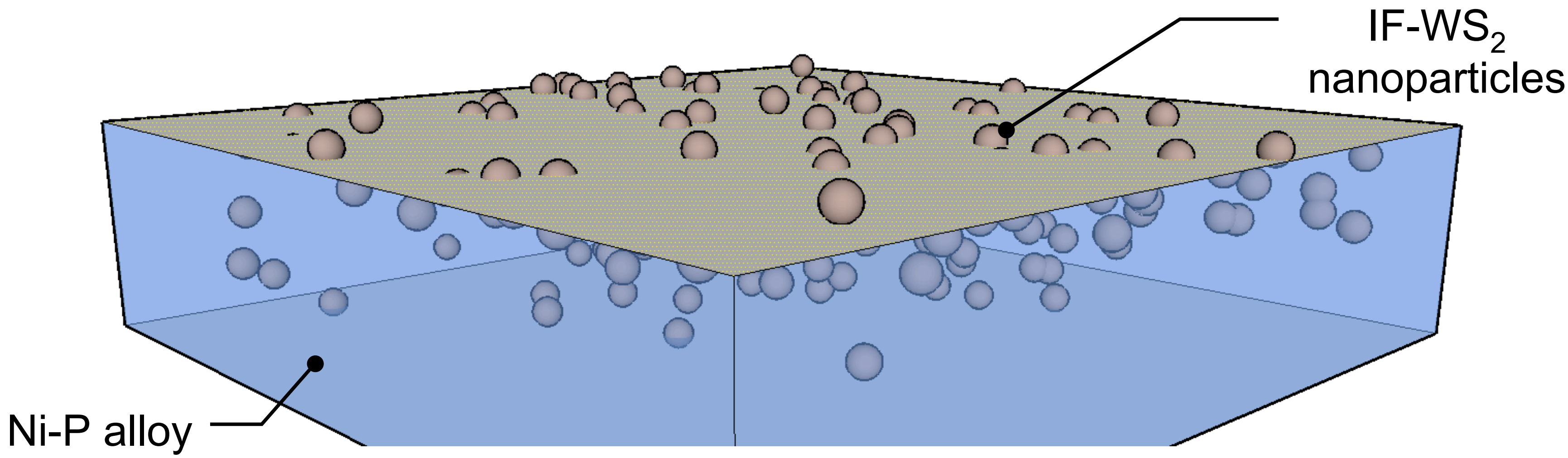

3D Model of the Solid Lubricant Thin Film

Coating	Mass loss of block [mg]	Friction Coefficient
Ni-P	15.6	0.090
Ni-P-(2H-WS_2)	5.2	0.062
Ni-P-Graphite	4.3	0.067
Ni-P-(IF-WS_2)	**3.0**	**0.030**

Results of Wear and Friction Coefficient

(Ref. [7])

An Electroless Ni-P-(IF-WS_2) Composite Coating

1. Nickel sulfate: 20-25 g/L
2. Sodium hypophosphite: 20-25 g/L
3. Sodium acetate: 10-15 g/L
4. Acetic acid: 5-10 mL/L
5. Surface agent: 200-400 mg/L
6. IF-WS_2 Nanoparticles: 6 g/L
7. pH: 4.5 - 5.1
8. Temperature: 80 - 85 °C
9. First a Ni-P coating is deposited for 0.5 h
10. Then Ni-P-(IF-WS_2) coating is deposited for 2.5 h
11. Annealing for 2 h at 673 °K in vacuum furnace (Ref. [7])

Simulation Results

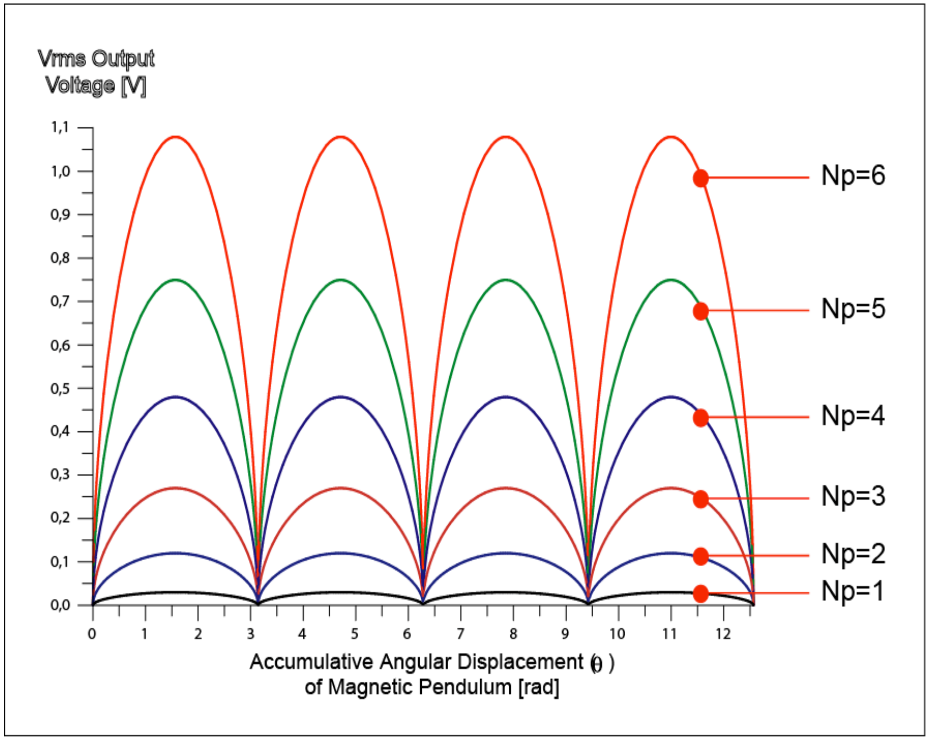

Generated Voltage Waveform

The graph shows the quadratic relationship between the output voltage and the angular displacement for different number of magnetic pole pairs inserted in the pendulum

Generator Major Design Specifications

Parameter	Value	
	Small version	Large version
Generator footprint area	1 mm x 1 mm	2 mm x 2 mm
Magnetic pendulum thickness (μm)	100	100
Pendulum radius (μm)	500	1000
Airgap thickness (μm)	10	10
Coil Cross-section (W x T) (μm)	1 x 1	2 x 2
Number of coil turns under pendulum	259	259
Pendulum angular velocity (max.) (rad/s)	182	129
Total coil reistance (kΩ)	3	1.5
Number of pole pairs in pendulum	6	6
Maximum energy product of thin film NdFeB	190 kJ/m^3	190 kJ/m^3
RMS output voltage (volts)	1.1	3.0
RMS power	390 μW	6.25 mW

Deposition of NdFeB thick films

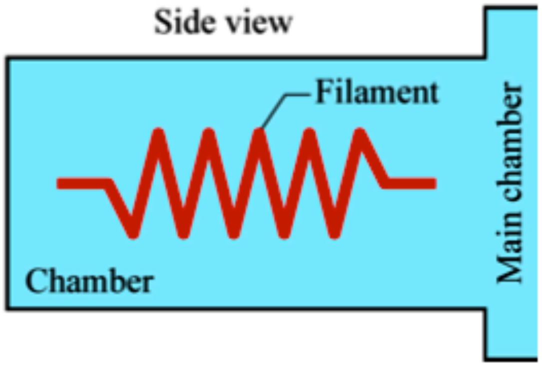

Titanium sublimation vacuum pump for oxidation suppresion

NdFeB by Pulsed Laser Deposition

- Deposition rates up to 50 µm / hour
- Remanence up to 1.5 T
- Closely similar composition of target material and prepared films.
- Laser outside chamber allows quick experimentation of laser types and parameters
- Oxidation must be suppressed to preserve magnetic properties

(Ref. [8,10])

Deposition of NdFeB thick films

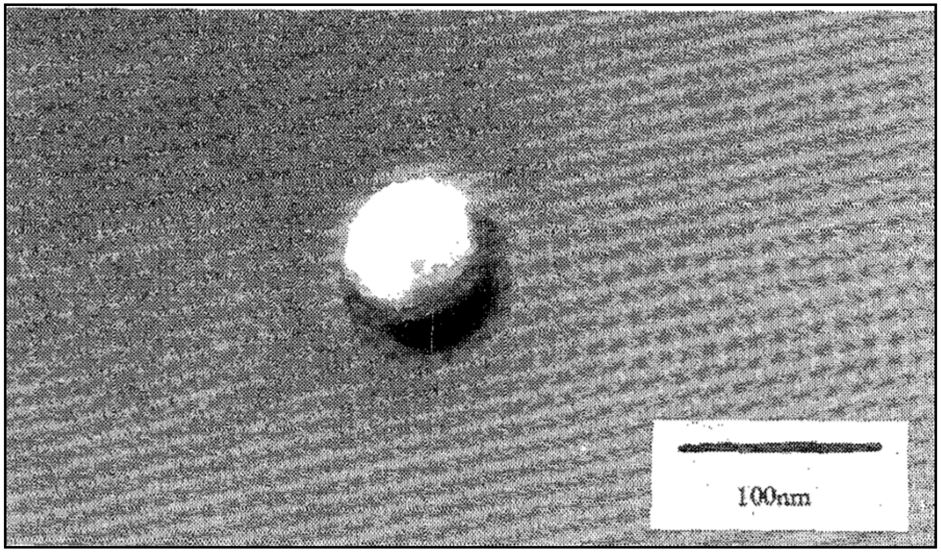

Ferrite alpha iron (αFe) droplets on NdFeB film caused by splashing effect of laser ablation.

Drawbacks of PLD technique

- Splashing effect
- Substrate must be heated, NdFeB film must be annealed at 600°C.
- Films are uniform over a small central area of substrate
- These disadvantages can be overcome (Ref. [8,10])

Micromachining of NdFeB films

NdFeB is a finely grained strongly bonded nanostructured material highly sensitive to corrosion

Standard photolithography

- Sputter deposited films of thickness up to 10µm can be patterned
- Etchants are nitric acid (HNO_3) and other highly oxidizing agents.
- Long exposure to etchant deteriorates magnetic properties
- Thick films cannot be patterned with oxidizing etchants

(Ref [8,9])

Micromachining of NdFeB films

Laser micromachining

- Almost any material can be patterned
- Preserves chemical composition and magnetic properties
- Tight tolerance features from a few µm are obtained
- Readily available
- High peak-power short pulses at high pulse repetitions can overcome hardness and transparency of materials.
- No surface pre-treatment is necessary

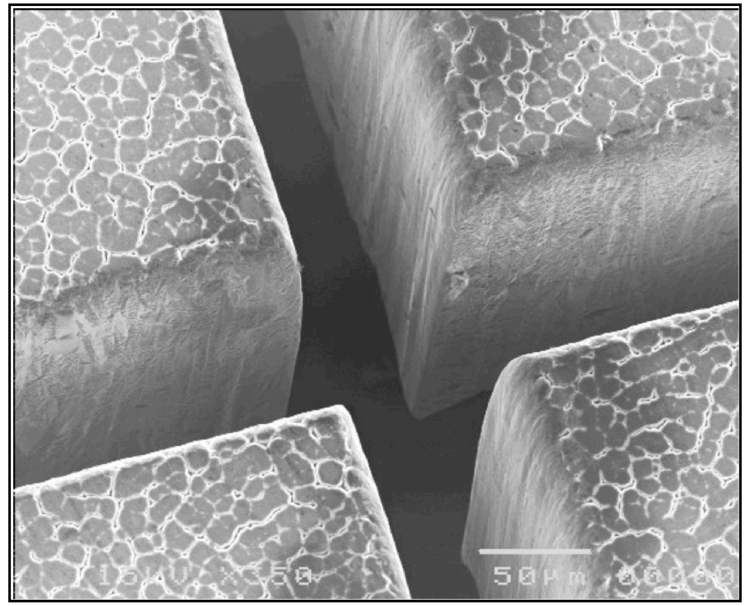

Laser machined CVD diamond film

In any case corrosion protective coating must be applied immediately after machining

(Ref [8,9])

Fabrication

1.

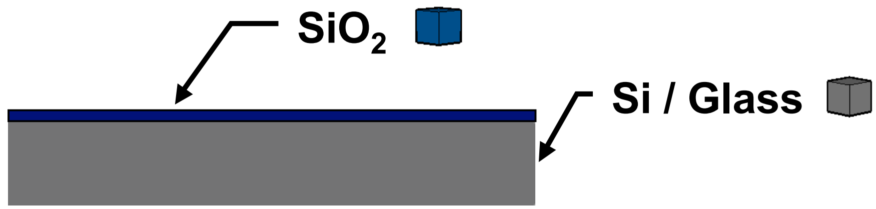

A thermally grown silicon dioxide layer is deposited on top of a <100> Silicon or glass substrate.

2.

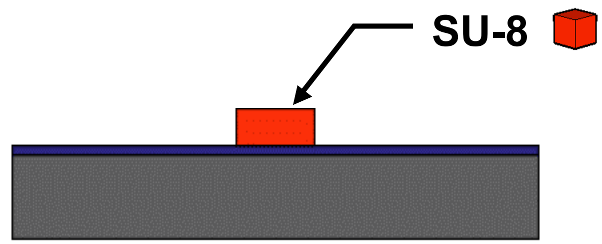

A 10 μm thick cylinder is patterned in SU-8 to act as a spacer between the rotor pendulum and the copper coil,

3.

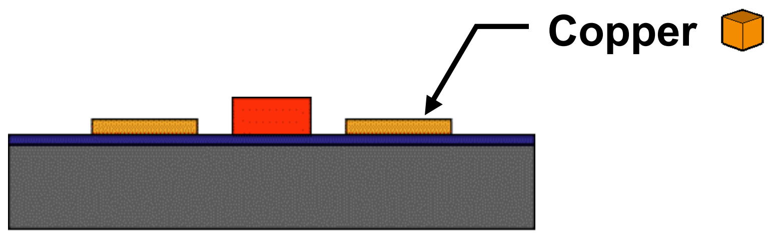

A 1.0 μm thick copper layer is sputter deposited and patterned to form the planar coil geometry.

4.

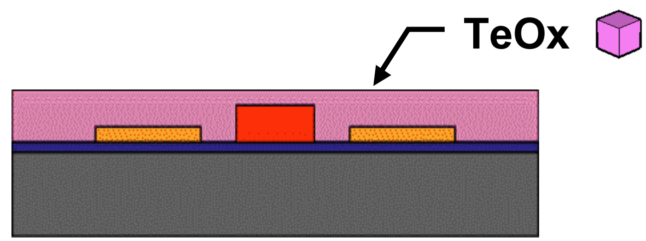

A 13 μm thick layer of TeOx sacrificial material is deposited over the copper coil and spacer.

Fabrication

5.

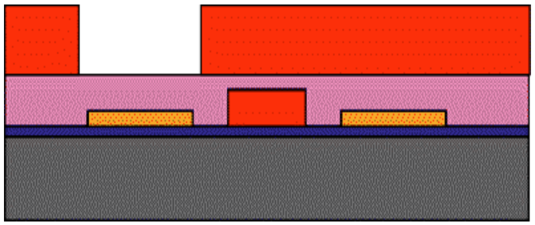

A 100 μm thick layer of SU-8 is spin deposited and through-etched for subsequent deposition of NdFeB.

6.

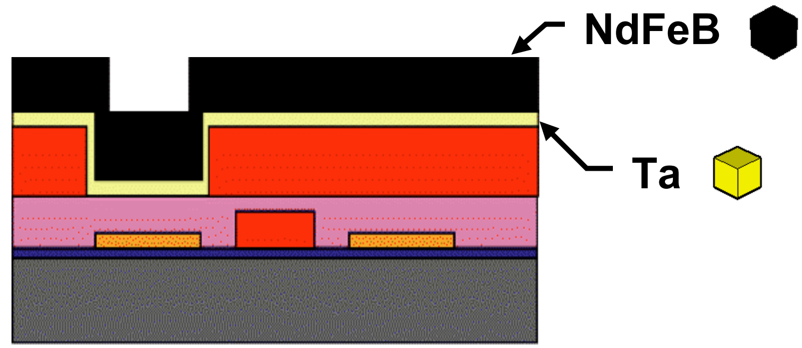

A thin layer of Tantalum is sputter deposited to act as an adhesion layer for NdFeB. Then, a 100 μm thick NdFeB film is deposited by pulsed laser deposition (PLD) method.

7.

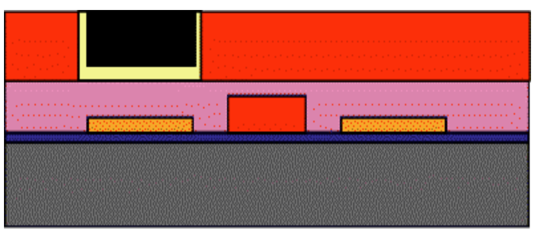

A procedure of planarization eliminates the remaining material, exposing the layer of SU-8 again.

8.

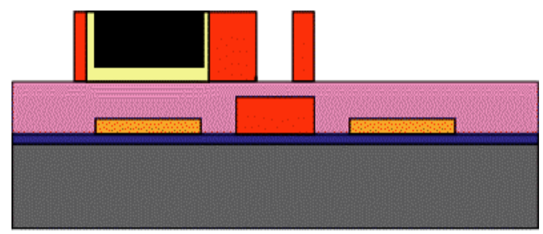

The SU-8 layer is patterned to create the semicircular pendulum-shaped geometry.

Fabrication

9.

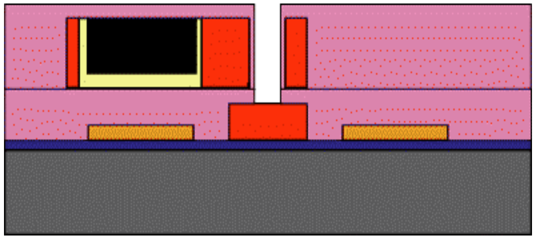

A SiO_2 sacrificial layer is deposited and trenched down to the spacer, leaving a thin film of sacrificial material coating the inner walls of the trench.

10.

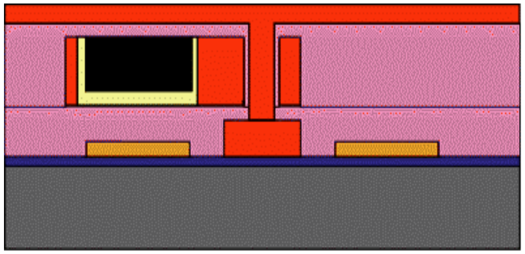

To form the shaft, a new layer of SU-8 is deposited. The material fills up the trench and reaches the spacer of the same material.

11.

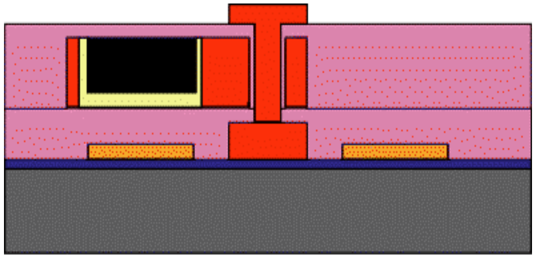

The last feature is patterned on the SU-8 layer to build a cap that holds the pendulum in place.

12.

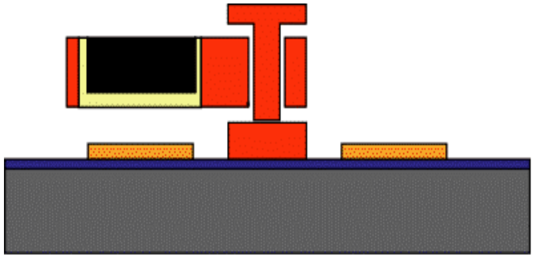

The sacrificial material is dissolved, enabling the pendulum to rotate freely around the shaft.

Packaging and Mounting

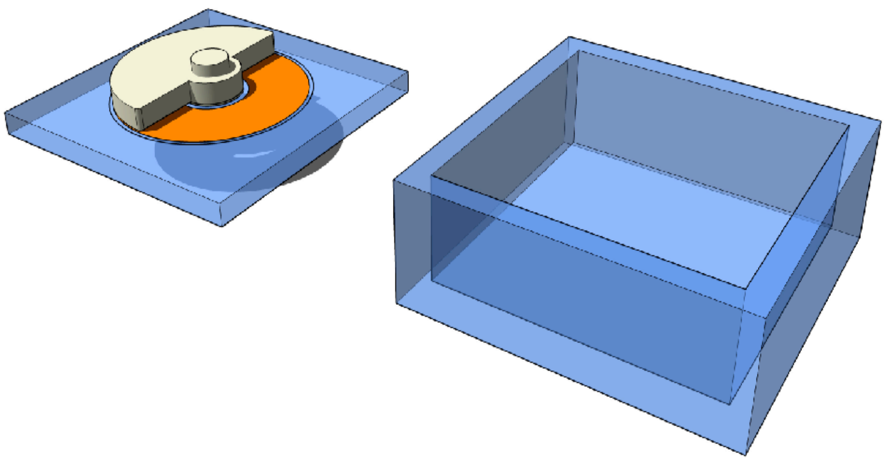

Electromagnetically shielded vacuum sealed package will ensure biocompatibility

A three-axes mounting system will ensure power generation at any physical posture of a person (e.g., standing or laying down on back or on a side)

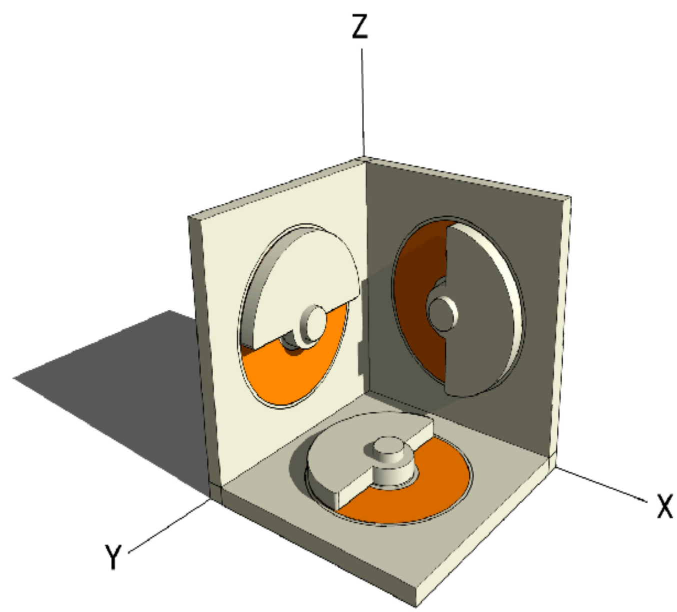

Future Directions

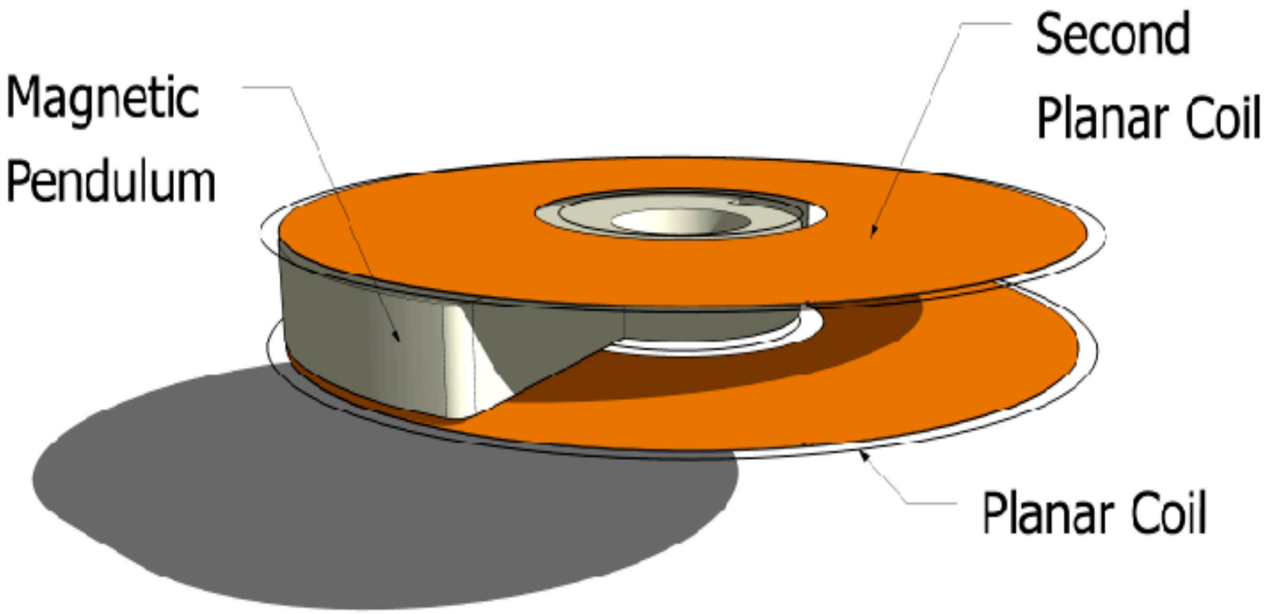

Two-Coil Microgenerator will be able to generate more power per unit volume

Future Directions

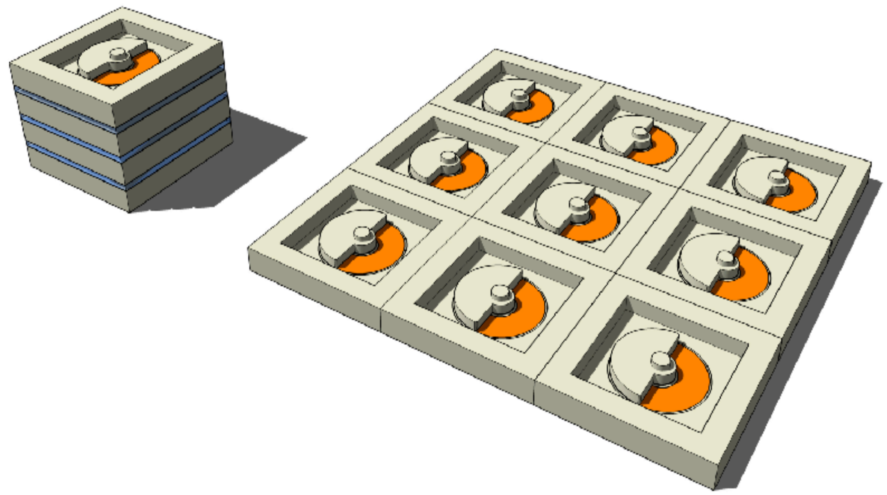

- Stacks and Arrays of microgenerators will enable to meet higher power demands and fit in a broad number of applications.
- On-board power level sensing: more generators would be cut in to the system by a control circuit if voltage falls below a threshold value.
- Built-in MEMS supercapacitors: energy storage will ensure power availability for the target device over periods of inactivity.

Conclusions

- The design of a novel MEMS-based axial flux micro power generator for implantable biomedical devices has been presented with a focus on cardiac pacemaker applications
- In the system, a semicircular magnetic pendulum oscillates around a central shaft due to body motion, for example, the thorax movement during breathing or head turning, to induce a voltage across an underlying copper coil
- A 1 mm^2 footprint area device can generate 390 μW of power with an open circuit RMS voltage of 1.1 volts
- Scaled or stacked versions can be used to satisfy power requirements for other implantable device applications
- The device can provide a greater energy supply per unit volume compared to existing pacemaker batteries and can aid in developing smaller pacemakers
- Maintenance free longer life minimizes frequency of invasive surgery as necessary for conventional pacemaker replacement due to battery exhaust.
- Further development of the device is in progress

Acknowledgements

The authors would like to greatly acknowledge the generous supports provided by:

- Natural Sciences and Engineering research Council of Canada (NSERC)
- CMC Microsystems, and
- IntelliSense Software Corporation of Woburn, MA

References

[1] M. Forde, P. Ridgely, “Implantable Cardiac Pacemakers”, in *The Biomedical Engineering Handbook*: Second Edition, Ed. Joseph D. Bronzino, Boca Raton: CRC Press LLC, 2000, Chapter 77, pp. 1-13.

[2] V. S. Mallela, V. Ilankumaran, and N.S. Rao, “Trends in Cardiac Pacemaker Batteries”, *Indian Pacing and Electrophysiology Journal*, vol. 4, no. 4, pp. 201-212, 2004.

[3] Perlo, et al., “Microgenerator of electrical energy”, *US Patent 6,932,030*, August 23, 2005; USA.

[4] A. S. Holmes, G. Hong, and K. R. Pullen, “Axial-Flux Permanent Magnet Machines for Micropower Generation”, *JMEMS*, Vol. 14, No. 1, pp. 54-62, February 2005.

[5] S. A. P. Haddad, R. P. M. Houben, and W. A. Serdijn, “The Evolution of Pacemakers”, *IEEE Engineering in Medicine and Biology Magazine*, pp. 38-48, May/June 2006.

[6] S. Das, D. P. Arnold, I. Zana, J.-W. Park, M. G. Allen, J. H. Lang, "Microfabricated High-Speed Axial-Flux Multiwatt Permanent-Magnet Generators—Part I: Modeling", *Journal of Microelectromechanical Systems*, Vol. 15, No. 5, October 2006.

[7] W. X. Chen, J. P. Tu, Z. D. Xu, R. Tenne, R. Rosenstveig, W. L. Chen, and H.i Y. Gan, “Wear and Friction of Ni-P Electroless Composite Coating Including Inorganic Fullerene WS_2 Nanoparticles", Advanced Engineering Materials 2002, 4, No. 9

References

[8] H. Lemke, C. Echer, and 6. Thomas, “Electrical Microscopy of Thin Films Prepared by Laser Ablation”, *IEEE Transactions on Magnetics*, Vol 32, No 5, September 1996.

[9] H. Lemke, T. Lang, T. Goddenhenrich, C. Heiden , “Micro patterning of thin Nd-Fe-B films”,, Journal of Magnetism and Magnetic Materials 148 (1995) 426-432.

[10] M. Nakano, R. Katoh, H. Fukunaga, S. Tutumi, and F. Yamashita, "Fabrication of Nd–Fe–B Thick-Film Magnets by High-Speed PLD Method”, IEEE Transactions on Magnetics, Vol. 39, No. 5, pp. 2863-2865, Sept. 2003.